

# Detection of extracellular matrix modification in cancer models with inverse spectroscopic optical coherence tomography

Graham L C Spicer<sup>1</sup>, Samira M Azarin<sup>2</sup>, Ji Yi<sup>3</sup>,  
Scott T Young<sup>4</sup>, Ronald Ellis<sup>1</sup>, Greta M Bauer<sup>4</sup>,  
Lonnie D Shea<sup>1,5,6</sup> and Vadim Backman<sup>4,7,8</sup>

<sup>1</sup> Department of Chemical and Biological Engineering, Northwestern University, Evanston, IL, USA

<sup>2</sup> Department of Chemical Engineering and Materials Science, University of Minnesota, Minneapolis, MN, USA

<sup>3</sup> Department of Medicine, Boston University, Boston, MA, USA

<sup>4</sup> Department of Biomedical Engineering, Northwestern University, Evanston, IL, USA

<sup>5</sup> Department of Biomedical Engineering, University of Michigan, Ann Arbor, MI, USA

<sup>6</sup> Department of Chemical Engineering, University of Michigan, Ann Arbor, MI, USA

<sup>7</sup> Chemistry of Life Processes Institute, Northwestern University, Evanston, IL, USA

<sup>8</sup> The Robert H. Lurie Comprehensive Cancer Center of Northwestern University, Chicago, IL, USA

E-mail: [v-backman@northwestern.edu](mailto:v-backman@northwestern.edu)

Received 17 December 2015, revised 13 July 2016

Accepted for publication 22 July 2016

Published 12 September 2016



## Abstract


In cancer biology, there has been a recent effort to understand tumor formation in the context of the tissue microenvironment. In particular, recent progress has explored the mechanisms behind how changes in the cell-extracellular matrix ensemble influence progression of the disease. The extensive use of *in vitro* tissue culture models in simulant matrix has proven effective at studying such interactions, but modalities for non-invasively quantifying aspects of these systems are scant. We present the novel application of an imaging technique, Inverse Spectroscopic Optical Coherence Tomography, for the non-destructive measurement of *in vitro* biological samples during



Original content from this work may be used under the terms of the [Creative Commons Attribution 3.0 licence](https://creativecommons.org/licenses/by/3.0/). Any further distribution of this work must maintain attribution to the author(s) and the title of the work, journal citation and DOI.

matrix remodeling. Our findings indicate that the nanoscale-sensitive mass density correlation shape factor  $D$  of cancer cells increases in response to a more crosslinked matrix. We present a facile technique for the non-invasive, quantitative study of the micro- and nano-scale structure of the extracellular matrix and its host cells.

Keywords: optical coherence tomography, extracellular matrix, cancer, nanoscale, STORM, phenotype

 Online supplementary data available from [stacks.iop.org/PMB/61/6892/mmedia](http://stacks.iop.org/PMB/61/6892/mmedia)

(Some figures may appear in colour only in the online journal)

## 1. Introduction

Colon cancer is the third-most prevalent cause of new cancer cases and cancer-related deaths in the US, with an estimated 93 090 new cases expected to be diagnosed in 2015 (American Cancer Society 2015). While screening methods have improved detection of colon cancer, many of the mechanisms governing disease progression remain poorly understood. Interactions between cells and the extracellular matrix (ECM) have been implicated in promotion of tumor growth and progression in many types of cancer (Nelson and Bissell 2006, Peddareddigari *et al* 2010, Cox and Erler 2011, Dvorak *et al* 2011, Lu *et al* 2012, Barcus *et al* 2013, Zou *et al* 2013, Chaudhuri *et al* 2014, Pickup *et al* 2014). In particular, matrix crosslinking has been shown to facilitate invasion and migration of tumor cells (Levental *et al* 2009, Fraley *et al* 2015). Collagen is a major constituent of the ECM in both normal colon tissue and colorectal tumors (Naba *et al* 2014). In the tumor microenvironment studies using second harmonic generation microscopy (SHG) have shown transformation of collagen structure in tumors compared to healthy tissue, with ECM in tumors displaying a higher orientation of collagen fibers and thicker fiber bundles indicative of crosslinking (Zhuo *et al* 2009, Nadiarykh *et al* 2010, Chen *et al* 2012).

Collagen crosslinking in the tumor microenvironment is believed to be catalyzed by the enzyme lysyl oxidase (LOX), which oxidizes lysine residues from collagen and elastin to form reactive semialdehydes (Butler *et al* 1987). LOX upregulation is associated with proliferation, invasion, and metastasis of breast cancer cells (Kirschmann *et al* 2002, Erler *et al* 2006, Cox *et al* 2013). Colon tumor tissues exhibit higher levels of LOX expression than normal colon tissue, with even greater increase in LOX expression for metastatic tumor tissues (Baker *et al* 2011). Another study using PCR found that upregulation of LOX, LOXL2, and LOXL4 was found in colorectal adenomas with absence of lymphovascular invasion, indicating oxygen tension dependent expression of these enzymes (Kim *et al* 2009). This suggests that LOXL2 and LOXL4 also contribute to the progression of colorectal cancer. In addition, LOX-mediated collagen crosslinking increases matrix stiffness to increase proliferation and invasiveness of colon cancer cells *in vitro* and *in vivo* (Baker *et al* 2012). Proliferation studies of early stage colorectal adenocarcinoma line SW480 and metastatic colorectal adenocarcinoma line SW620 cultured on 3D collagen matrices found increased cellular proliferation with LOX treatment to both SW480 and SW620 lines (Baker *et al* 2011).

Current techniques used to study the interplay between cells and matrix include migration assays to measure cellular motility through the ECM, and proliferation assays to measure cellular proliferation and metabolic activity (Kirschmann *et al* 2002, Erler *et al* 2006, Kim

*et al* 2009, Baker *et al* 2011, 2012, Tse *et al* 2012, Cox *et al* 2013). In addition, biochemical and genetic analyses have been used extensively to quantify differential gene expression and cell signaling. To complement these functional and biochemical studies, histology and microscopy techniques have been used for qualitative and pseudo-quantitative analyses of antigen localization and structural morphology of tissue and *in vitro* models (Kim *et al* 2009, Baker *et al* 2011, 2012, Conklin *et al* 2011, Barcus *et al* 2013, Cox *et al* 2013). Furthermore, the development of superresolution microscopy has enabled the direct visualization of nanoscale structures in and outside the cell, including actin, tubulin, mitochondria, and many ECM proteins. These recent advances have enabled much new insight into cellular structure at the nanoscale, leading to a better understanding of these complex systems and how their morphologic and chemical signaling leads to cancer progression. However, super-resolution microscopy techniques have very limited working distances and require introduction of molecular probes to label structures of interest, complicating sample preparation. The introduction of a technique sensitive to nanoscale changes such as superresolution microscopy with the capability to image a wide variety of unlabeled biological systems will be of great utility in further structural study of the complex interplay between cells and the ECM in cancer biology.

Inverse spectroscopic optical coherence tomography (ISOCT) is an emerging technique utilizing spectral domain OCT signal resampling to determine the backscatter intensity spectra at every voxel in a 3D OCT scan (Yi and Backman 2012). From this spectral information, ultrastructural parameters can be extracted to quantitatively characterize the sample. Specifically, by assuming tissue to be a continuous random medium, a mass density correlation parameter,  $D$ , can be obtained from the relation,  $\mu_b \propto k^{4-D}$ , where  $\mu_b$  is the backscattering coefficient, which is proportional to the squared OCT intensity, and  $k$  is the wavenumber, for each 3D OCT resolution voxel measuring  $8 \times 8 \times 4 \mu\text{m}$ . Physically, when  $D$  is less than 3, it represents a mass fractal dimension characteristic of the voxel being sampled. In previous studies with ISOCT, the length scale sensitivity of  $D$  has been established theoretically and experimentally to structures between 35 and 450 nm in size (Yi *et al* 2013). Measurement of *ex vivo* biopsies from patients with colorectal and pancreatic cancers showed ISOCT is sensitive to ultrastructural changes induced by field carcinogenesis, manifesting in higher  $D$  values measured from patients with cancer (Yi *et al* 2014). The fact that tissues associated with field carcinogenesis appear histologically normal is in agreement with the ISOCT observation that the associated structural modifications occur below the optical diffraction limit. Although they cannot be imaged by conventional microscopy, these alterations are still detectable with ISOCT (Slaughter *et al* 1953). While ISOCT is as limited as traditional OCT with regards to spatial resolution, its ability to detect structural changes at the nanoscale from spectral fitting lends it for non-invasive study of dynamic phenomena in biological systems that occur at length scales below the diffraction limit. The penetration depth and working distance of ISOCT, on the order of 1–2 mm, far surpasses the working distance of traditional optical microscopes. This enables rapid facile imaging of thick 3D cell cultures with minimal sample preparation.

Here, we demonstrate ISOCT as a valuable tool for the study of cell-ECM interactions in the context of a simple *in vitro* model. We show the sensitivity of ISOCT to enzymatic collagen crosslinking, as well as present it as a technique to study the structural phenotype of cells, as reflected by the response of colon cancer cells to a crosslinked collagen substrate. The increased proliferative phenotype adopted by colon cancer cells on a crosslinked collagen substrate is shown here to correlate with an increase in  $D$  measured from live cell colonies on collagen. Thus, the proliferative phenotype shift is accompanied by a nanoscale structural phenotype shift of cells in this model of cancer progression, a finding that will push forward

the development of optical screening strategies and testing of therapeutics to stem cancer progression.

## 2. Method

### 2.1. LOX treated collagen gels

Solutions of collagen were prepared by mixing rat-tail collagen I (BD Biosciences) with sterile dH<sub>2</sub>O water, 10X PBS (Sigma, 1:10 dilution), and 1 M NaOH (Sigma, 1:100 dilution) on ice. For all LOXL4 treated gels, LOXL4 (Sigma) was added to the freshly mixed collagen I solution to reach a final LOXL4 concentration of 350 ng ml<sup>-1</sup> prior to collagen gelation.

### 2.2. STORM imaging and analysis

For STORM imaging, collagen gel structures were labeled with Alexa Fluor 647 dye (Thermo Fisher) by directly mixing 1 aliquot of dye with 250  $\mu$ l of freshly prepared 2.5 mg ml<sup>-1</sup> collagen solution. After incubation for 1 h for gelation, dye was leached from gels by adding 1X PBS to gels, replacing every 24 h for 3 d. Imaging was performed on a Nikon STochastic Optical Reconstruction Microscope at the Northwestern Feinberg School of Medicine Nikon Imaging Center. 2D depth-sectioned STORM images were acquired from a depth within the collagen gel sample, away from the glass coverslip, with a lateral resolution of 50 nm. The spatial autocorrelation function,  $B_n(r)$ , of each STORM image was taken to be representative of the collagen fiber network mass density distribution, due to the absence of other scattering species within the sample. This function,  $B_n(r)$ , was fit to the Whittle–Matérn family of correlation function, whereby the fit parameter  $D$  was taken as a representative quantification of collagen mass density at the nanoscale resolution of STORM.

### 2.3. Cell culture

Human colon cancer lines HT-29 (primary tumor) and SW620 (metastatic site) were cultured in McCoy's 5A (Thermo Fisher, Carlsbad, CA) and Dulbecco's Modified Eagle media (Sigma, St. Louis, MO), respectively, substituted with 10% fetal bovine serum. Cells were grown in a 5% CO<sub>2</sub> environment at 37 °C and split upon reaching 80% confluency.

### 2.4. WST-1 proliferation assay

To quantify cellular proliferation as a marker of phenotype induced by matrix crosslinking, HT-29 and SW620 human colon cancer cell lines were split and seeded on top of collagen gels prepared as described above. 50  $\mu$ l of the collagen solution having LOXL4 concentrations of either 0 or 350 ng ml<sup>-1</sup> was added to each well of a 96 well plate. The collagen-coated wells were incubated for 1 h at 37 °C to allow for gelation, then 150  $\mu$ l of split cells in media was added to each well. After 2 d incubation, media was replaced with fresh media containing WST-1 (4-[3-(4-iodophenyl)-2-(4-nitrophenyl)-2H-5-tetrazolio]-1, 3-benzene disulfonate) reagent (Sigma, St. Louis, MO). After 30 min incubation at 37 °C with WST-1, the absorbance of the plate was read at 440 nm in a Synergy H1 Multi-Mode plate reader at the Northwestern Recombinant Protein Production Core. After measurement, the plate was incubated for an additional 15 min before additional measurement. Cell proliferation is directly related to the difference in absorbance between the second measurement, taken at 45 min, and the first measurement, taken at 30 min.

### 2.5. ISOCT study of cellular phenotype

For ISOCT study of cellular phenotype dependence on ECM structure, collagen gels were made in an 8-well chamber slide (Thermo Fisher Scientific) with  $1.6 \text{ mg ml}^{-1}$  collagen concentration. Gels were incubated at  $37^\circ \text{C}$  for 24 h prior to seeding cells on the surface of the gel. After seeding, cells were incubated for 6 d prior to imaging with ISOCT in chamber slides.

ISOCT imaging was conducted on an instrumental setup described in references (Yi and Backman 2012, Yi *et al* 2014). Briefly, the instrument consisted of a traditional spectral domain OCT system utilizing a supercontinuum laser source (NKT Photonics) for illumination and a spectrometer with spectral coverage from 650 to 820 nm over a 2048 pixel CMOS camera. OCT scans of  $256 \times 256$  A-lines were acquired at 2560 Hz over a  $2 \times 2$  mm scan area, giving a B-scan rate of 10 frames per second. The axial and lateral resolutions of the system were approximately  $1.5 \mu\text{m}$  and  $10 \mu\text{m}$ , respectively, with an effective NA of 0.04. ISOCT data collected from cell samples was normalized using an aqueous suspension of 80 nm polystyrene spheres as a Rayleigh scattering reference medium with backscattering coefficient  $\mu_b$  proportional to  $k^4$ . 3D spatially resolved mass density correlation functional factor,  $D$ , was calculated from this relation with a voxel edge length of  $4 \mu\text{m}$  axially and  $8 \mu\text{m}$  laterally, using 7 separate spectral resampling windows in a wavelength range from 674 to 754 nm.

To perform 3D segmentation of cells from their collagen substrate, regions of interest (ROIs) were manually drawn on *en face* projections of the 3D OCT spatial intensity maps generated by each OCT scan. These ROIs were used to select areas of the collagen substrate covered by cellular colonies. OCT B-scans of cell layers on collagen were surveyed to determine a characteristic thickness of these layers. An edge detection algorithm was used to find the height of the top surface of the cell layer. Taking into account a pixel buffer below the detected edge to the bright cell layer for both cell lines, 3D ROIs were generated by extruding the manually segmented lateral ROI along the  $z$ -dimension between 2–15 pixels and 2–10 pixels for HT-29 and SW620 cell lines, respectively, corresponding to the characteristic thicknesses of  $56 \mu\text{m}$  and  $36 \mu\text{m}$  for these lines determined from the survey of OCT B-scans. An example OCT B-scan of an HT29 cell layer on top of collagen with corresponding upper and lower pixel bounds is shown in figure S1 ([stacks.iop.org/PMB/61/6892/mmedia](http://stacks.iop.org/PMB/61/6892/mmedia)) in the supplementary material. Mean  $D$  values for cellular colonies in each scan were computed as the arithmetic mean of all  $D$  values for voxels within the 3D ROI.

### 2.6. Confocal imaging of HT-29 colonies on collagen

For confocal imaging of live HT-29 colonies and their interaction with their collagen substrate,  $100 \mu\text{l}$  of collagen solution ( $1.6 \text{ mg ml}^{-1}$ ) was used to coat the coverslip of a 35 mm glass bottom culture dish. Collagen was allowed to gel for 24 h at  $37^\circ \text{C}$  prior to seeding the gel with split HT-29 cells in media. After allowing cells to culture for 2 d,  $10 \mu\text{g ml}^{-1}$  Hoechst dye was added to cell media, after which cells were incubated for 2 h to ensure thorough nuclear staining. For confocal imaging, media was removed and cells were rinsed and covered with  $1 \times$  PBS. Confocal fluorescence microscopy was performed on an upright Leica TCS SP5 laser scanning confocal microscope system, with a  $20 \times$  water immersion objective imaging through PBS covering cells from the top. Confocal reflectance images were acquired simultaneously using 488, 496, and 514 nm lasers, in conjunction with a 405 nm laser for Hoescht fluorescence excitation.

### 3. Results and discussion

#### 3.1. Ultrastructural study of crosslinked collagen gel

In order to visualize the structural effects of LOXL4-induced crosslinking of collagen, stochastic optical reconstruction microscopy (STORM), with a transverse resolution of 40 nm, was used to image collagen gels, untreated and treated with 350 ng ml<sup>-1</sup> of LOXL4, a concentration reflective of LOX expression in rat connective tissues (Rucker *et al* 1998). Representative images of collagen gels from each group are shown in figures 1(A) control and (B) LOXL4 treated. In the gel treated with LOXL4, crosslinking manifests in thicker fibrous structures throughout the gel, and sporadic bundles of thick fiber bundles. To quantify this characteristic clumping of the collagen fiber network from STORM images, the autocorrelation function of the full image was computed and its radial average was fit to the Whittle–Matérn model of autocorrelation functions. Examples of Whittle–Matérn fit of the image autocorrelation for control and crosslinked collagen samples are presented in figure S2 in the supplementary material. The fit parameter  $D$ , corresponding to the shape of the optical backscattering spectrum, was averaged from 4 independent images of collagen gels in each group. Average  $D$  values from STORM images are presented in figure 1(C).

ISOCT was used to measure gels prepared identically to those imaged with STORM. ISOCT spectral signal was averaged from a manually selected region of interest from the *en face* projection of each OCT scan, and the mean  $D$  value for the scan was calculated from the fit of this averaged intensity spectrum. Results were taken as the mean of 30 independent scans of collagen gel from each group, shown in figure 1(D). ISOCT detected a similar increase in  $D$  when comparing LOXL4 treated gels to the untreated control gel group. While the value of  $D$  determined by STORM compared to ISOCT differs when comparing groups, this could be attributable to the different measurement techniques introducing differing systematic errors to this measurement. Since ISOCT has been rigorously validated to establish the accuracy of  $D$  values measured from polystyrene bead phantoms, we believe this difference to arise due to the labeling accuracy of STORM images, which reflect the distribution of fluorescent dye molecules and not necessarily all collagen structures which scatter light (Yi and Backman 2012, Yi *et al* 2013). Furthermore, the isotropy of a collagen gel network lends itself to quantification of  $D$  from ISOCT signal, regardless of illumination direction. This isotropy allows for direct comparison of ultrastructural parameters measured in the transverse sample plane by STORM with measurements taken in the axial dimension with ISOCT.

#### 3.2. Measuring progression of crosslinking with ISOCT

Further study of the crosslinking of collagen gel as a time course experiment was conducted to demonstrate how the  $D$  value of collagen gel changes as the collagen changes from a transparent liquid solution to the weakly scattering gel used in these studies. This gelation is induced by the mixing of sodium hydroxide with the collagen solution to lower the pH, enabling hydroxylation and covalent crosslinking of tropocollagen molecules into a collagen microfibril network. As this reaction proceeds, an increase in  $D$  is expected as fibers aggregate into larger bundles with a higher spatial autocorrelation. Results from this time course experiment are presented in figure 2.

#### 3.3. Cancer cell phenotype induced by ECM

To study the effect of enzymatic matrix crosslinking on cellular phenotype in cancer, human colon cancer lines HT-29 (primary tumor) and SW620 (metastatic site) were used to model this interaction. Cells were seeded on top of hydrated collagen gels prepared similarly to those used for STORM study, with the omission of Alexa 647 dye. After culturing the cells on the

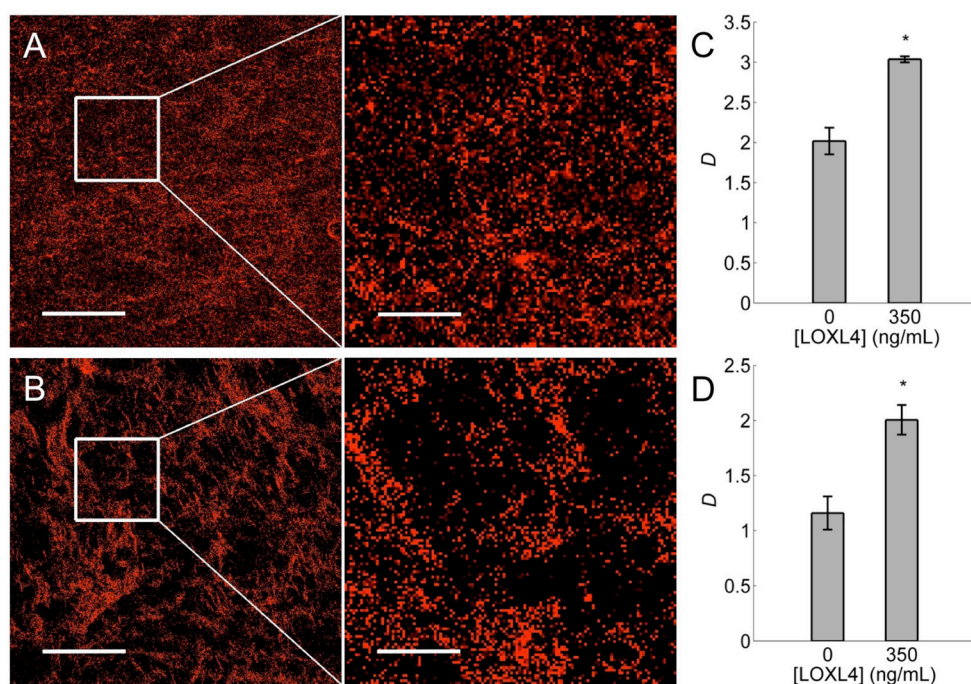


**Figure 1.** STORM images of (A) control and (B) LOXL4-treated collagen gel samples (scale bar length is 10  $\mu\text{m}$ ). (C)  $D$  values computed from Whittle–Matérn fit of STORM image autocorrelation functions ( $*p < 0.01$ ,  $N = 4$  per bar). (D)  $D$  values measured with ISOCT from gels prepared in the same manner as those used for STORM imaging ( $*p < 0.0001$ ,  $N = 30$  per bar).

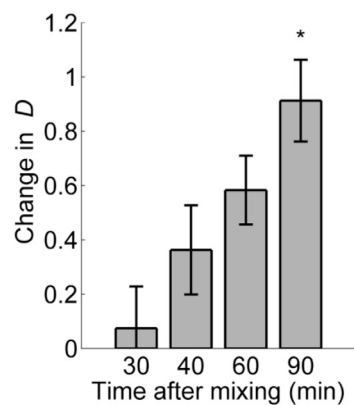


**Figure 2.** Results of time course experiment designed to measure ultrastructural changes in collagen gel with ISOCT as the gel solidifies and crosslinks. ISOCT non-invasively probes the bulk gel to measure change in  $D$  compared to initial measurement at 20 min ( $*p < 0.001$  comparing 20 and 90 min time points,  $N = 6$  per bar).

collagen gel substrates for two days, a WST-1 assay was performed on the cells to quantify the degree of proliferation during the two-day culture period. The assay revealed significant increase ( $p < 0.001$ ) in proliferation of both HT-29 and SW620 cells when cultured on collagen crosslinked with LOXL4, compared to control as shown in figure 3.

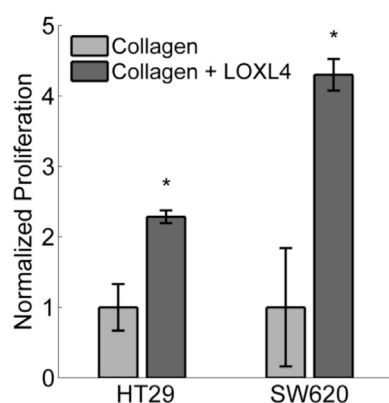


**Figure 3.** Results of WST-1 Assay performed on HT-29 and SW620 cell lines cultured on collagen gels to detect proliferative phenotype shift ( $*p < 0.001$ ,  $N = 24$  per bar).

### 3.4. Measuring structural phenotype of cancer cells with ISOCT

ISOCT was used to measure the same cell-ECM model system used for WST assay study. Normal culture media was removed from cell beds cultured on collagen in an 8-well chamber slide, and cell beds were quickly scanned with ISOCT. The results of this study of structural cellular phenotype are presented in figure 4, representing data taken from a single experimental run (sample size  $n = 3$ ). Two additional runs of the experiment verified these results with similar trends being shown for all trials. We observe a significant ( $p < 0.05$ ) effect of LOXL4-conditioned collagen substrate on the  $D$  value of cells when compared to the control collagen without LOXL4 induced crosslinking. This is indicative that matrix crosslinking has a positive effect on the  $D$  value and respective phenotype of HT-29 cells growing on a collagen substrate.

The 3D imaging ability of OCT enable the visualization of individual colonies of HT-29 cells growing on the collagen. This capability was used to determine cellular confluency of HT-29 colonies within the transverse 2 mm square scan area taken for ISOCT analysis. Manual segmentation of these colonies from the *en face* projection of the 3D OCT image cube yielded a significantly higher confluency of HT-29 colonies when grown on collagen treated with LOXL4 compared to the control collagen gel. This corroborates the finding that these cells proliferate more when cultured on the more crosslinked collagen substrate. To better visualize cell and collagen morphology with high resolution, confocal fluorescence microscopy was used with Hoechst dye to label cell nuclei. A superimposed confocal fluorescence image of the Hoechst channel with confocal reflectance microscopy to show collagen structure underlying live HT-29 colonies on collagen is presented in figure 5(A). In addition, an animation of a rotating confocal scan of this system is presented in video S3 in the supplementary material. For comparison with ISOCT as a quantitative imaging technique, an ISOCT B-scan of a highly confluent cell bed, color-coded by  $D$  value, is shown in figure 5(B).

We present here a study of enzymatic collagen crosslinking using ISOCT to show how this prevalent effect in carcinogenesis manifests in changes in nanostructure and ISOCT signal. The effects of LOX-catalyzed crosslinking of collagen have been well described by matrix stiffness and SHG measurements on tissues and *in vitro* models (Stoller *et al* 2002, Levental *et al* 2009, Chen *et al* 2012). We extend this study to the nanoscale, using



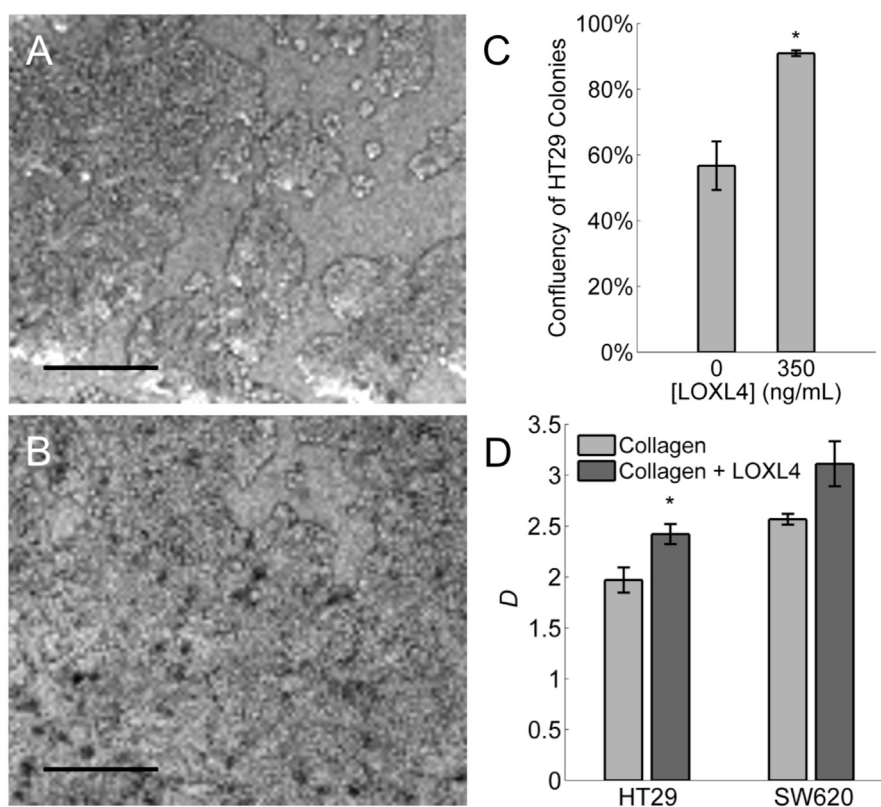


**Figure 4.** OCT *en face* projection images of HT-29 colonies cultured on top of (A) untreated and (B) LOXL4-treated collagen gels. Scale bar length = 250  $\mu\text{m}$ . (C) Confluency of HT-29 colonies was greater when cultured on collagen gel crosslinked with LOXL4 ( $*p < 0.05$ ,  $N = 3$  per bar). (D) ISOCT *D* values measured from cell colonies of lines HT-29 and SW620 *in situ* on *in vitro* collagen gel ( $*p < 0.05$ ,  $N = 3$  per bar). Cell layers segmented manually to ensure measurement signal taken from cells without interference from collagen.

STORM microscopy to resolve previously unobserved nanoscale structure of a hydrated collagen network and its response to LOXL4-mediated crosslinking. By calculating the correlation function shape parameter *D* from STORM images, we were able to parameterize the extent of crosslinking of collagen gels quantitatively. For *D* values between 0 and 3, *D* represents the mass fractal dimension of the sampled medium, a quantitative value reflective of the relative clumping of its statistical mass density. With increased crosslinking of collagen fibrils, *D* from the fibrous collagen network will increase. ISOCT measurement of the same collagen gel system revealed a similar effect size of LOXL4 crosslinking of the collagen gel when compared to the difference in *D* values between groups measured from STORM images. After confirming the sensitivity of ISOCT to collagen crosslinking, we demonstrated its applicability to longitudinal study of increasing *D* in a crosslinking collagen gel. While this is a simple model, it is a novel extension of ISOCT, demonstrating for the first time non-invasive nanoscale-sensitive study of structural modification of unlabeled hydrated collagen. This will lead to further study of animal models to study how collagen modifications occur in the earliest stages of carcinogenesis, as well as utilizing the

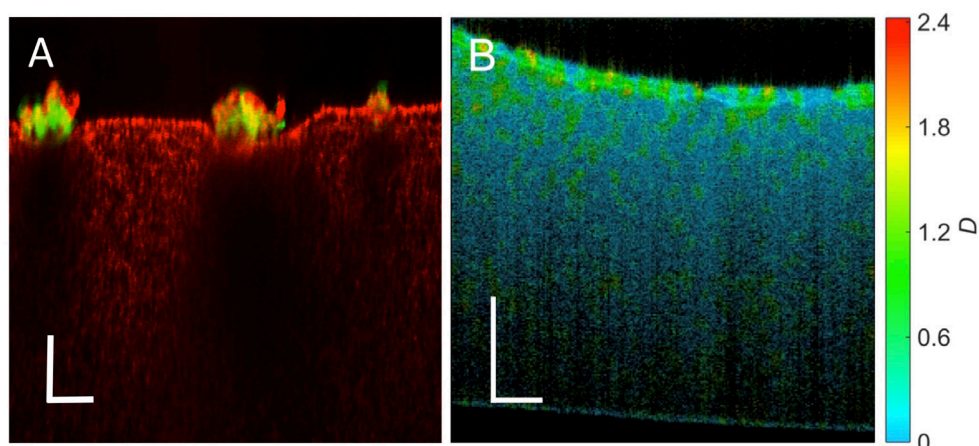


**Figure 5.** (A) Confocal fluorescence cross section of live HT-29 cell colonies cultured on collagen gel, nuclei shown in green and collagen shown in red. Scale bar length =  $50\ \mu\text{m}$ . (B) Example OCT B-scan of HT-29 colony cultured on top surface of collagen gel. Image brightness is scaled by OCT intensity and color is scaled by ISOCT parameter,  $D$ . The bright layer near the top of the frame is the HT-29 colony, with the substrate collagen underneath showing as a fainter homogeneous media. Scale bar length =  $250\ \mu\text{m}$ .

3D resolution of ISOCT to localize regions of ECM modification in tissue to optimize site-specific cancer screening with ISOCT.

We extended this model of collagen crosslinking in cancer to study how the crosslinked matrix affects cellular phenotype. When two commonly used colon cancer cell lines, HT-29 and SW620, were cultured on these collagen gel substrates, cells on the more crosslinked substrate showed a markedly higher proliferation and confluency, a shift in phenotype in line with previous behavioral studies such as migration and proliferation assays, as well as *in vivo* tumor models (Baker *et al* 2011). The results obtained here show the multimodality of ISOCT, with regards to its ability to resolve cellular localization and confluency in a live culture and demonstrate its potential for further study of more advanced 3D cell culture models.

To study the nanoscale differences in cells cultured on collagen gels, we quantified the cellular nanostructure and organization ( $D$ ) using ISOCT. We demonstrated ISOCT to be a facile non-invasive technology for the study of structural phenotype of cells to complement the established imaging capabilities of traditional OCT. ISOCT is sensitive to changes in cellular structure leading to an increased  $D$  value when cells are cultured on a more crosslinked matrix. Based on previous studies that determined the length scale sensitivity of  $D$  to be between 35 and 450 nm, the higher  $D$  associated with cells on a stiffer matrix likely arise due to changes in nuclear chromatin structure but may also be attributable to changes in the cytoskeleton, cellular organelles, or membrane structures (Yi *et al* 2013).

Previously, a study from our lab has identified dysregulated condensation of nuclear chromatin to be a diagnostic marker in the identification of early colon field carcinogenesis (Stypula-Cyrus *et al* 2013). Furthermore, these chromatin alterations via histone acetylation were detected by ISOCT (Yi *et al* 2015). Therefore, due to the relatively large scattering signature from the cell nucleus, the higher  $D$  measured from cells on crosslinked collagen could be attributable to such changes in the nuclear chromatin. Further studies are being pursued to

determine dominant structural effects underlying the change in  $D$  in these models, and will better explain the biological meaning of ISOCT signal, establishing ISOCT as an unparalleled technique in studying cellular nanostructure due to its superior depth of field and imaging speed when compared with superresolution microscopy.

Moreover, it has been well established that cells growing on a stiffer substrate adapt to this environment through mechanotransduction pathways, resulting in an altered cytoskeleton and cellular shape. While the HT-29 and SW620 cell lines studied here do not typically have a large cellular space outside of the nucleus, the higher elastic modulus of crosslinked collagen would likely have an effect on the cytoskeleton and glycoprotein adherence to the gel. Cytoskeletal disruption in isolated rat colonocytes has been shown to have a profound influence on optical scattering spectra derived ultrastructural parameters, indicating the possibility of a similar effect from cytoskeletal modification in this cell model (Mutyal *et al* 2013).

#### 4. Conclusions

In this study, we have used ISOCT to measure the nanoscale sensitive mass density correlation parameter  $D$  from living cell cultures. ISOCT is also presented as a tool to monitor an evolving system of collagen crosslinking, tracking the increase in  $D$  from a collagen gel as collagen molecules and microfibrils covalently crosslink during gelation. This capability of ISOCT to non-invasively probe living and evolving systems for 3D spatially resolved sub-diffractive nanoscale structural information is novel in the field of biomedical optics, and introduces a technique to address the tantalizing scientific puzzle of nanoscale dynamics in a native biological system. By harnessing the complementary information obtained from the 3D imaging of traditional OCT and the nanoscale-sensitive structural measurements of ISOCT, we anticipate this technique to be of great utility in further study of cell-ECM interactions and cancer screening. Future work will elucidate specific mechanisms of ECM modification in cancer, using ISOCT to probe subtle nanoscale changes in structure *in vitro* and *in vivo*.

#### Acknowledgments

The authors would like to acknowledge Luay Almassalha and Yolanda Stypula-Cyrus for their help in reviewing the manuscript. This work was supported by NIH R01 CA173745 and R01 CA183101 and NSF grant CBET-1240416. STORM imaging work was performed at the Northwestern University Center for Advanced Microscopy generously supported by NCI CCSG P30 CA060553 awarded to the Robert H Lurie Comprehensive Cancer Center.

#### References

- American Cancer Society 2015 *Cancer Facts and Figures 2015* (doi: [10.3322/caac.21254](https://doi.org/10.3322/caac.21254))
- Baker A-M, Bird D, Lang G, Cox T R and Erler J T 2012 Lysyl oxidase enzymatic function increases stiffness to drive colorectal cancer progression through FAK *Oncogene* **32** 1863–8
- Baker A-M, Cox T R, Bird D, Lang G, Murray G I, Sun X-F, Southall S M, Wilson J R and Erler J T 2011 The role of lysyl oxidase in SRC-dependent proliferation and metastasis of colorectal cancer *J. Natl Cancer Inst.* **103** 407–24
- Barcus C E, Keely P J, Eliceiri K W and Schuler L A 2013 Stiff collagen matrices increase tumorigenic prolactin signaling in breast cancer cells *J. Biol. Chem.* **288** 12722–32
- Butler E, Hardin J and Benson S 1987 The role of lysyl oxidase and collagen crosslinking during sea urchin development *Exp. Cell Res.* **173** 174–82

- Chaudhuri O, Koshy S T, Branco da Cunha C, Shin J, Verbeke C S, Allison K H and Mooney D J 2014 Extracellular matrix stiffness and composition jointly regulate the induction of malignant phenotypes in mammary epithelium *Nat. Mater.* **10** 1–9
- Chen X, Nadiarynk O, Plotnikov S and Campagnola P J 2012 Second harmonic generation microscopy for quantitative analysis of collagen fibrillar structure *Nat. Protocols* **7** 654–69
- Conklin M W, Eickhoff J C, Riching K M, Pehlke C A, Eliceiri K W, Provenzano P P, Friedl A and Keely P J 2011 Aligned collagen is a prognostic signature for survival in human breast carcinoma *Am. J. Pathol.* **178** 1221–32
- Cox T R, Bird D, Baker A-M, Barker H E, Ho M W-Y, Lang G and Erler J T 2013 LOX-mediated collagen crosslinking is responsible for fibrosis-enhanced metastasis *Cancer Res.* **73** 1721–32
- Cox T R and Erler J T 2011 Remodeling and homeostasis of the extracellular matrix: implications for fibrotic diseases and cancer *Dis. Models Mech.* **4** 165–78
- Dvorak H F, Weaver V M, Tlsty T D and Bergers G 2011 Tumor microenvironment and progression *J. Surg. Oncol.* **103** 468–74
- Erler J T, Bennewith K L, Nicolau M, Dornhöfer N, Kong C, Le Q-T, Chi J-T A, Jeffrey S S and Giaccia A J 2006 Lysyl oxidase is essential for hypoxia-induced metastasis *Nature* **440** 1222–6
- Fraley S I, Wu P, He L, Feng Y, Krisnamurthy R, Longmore G D and Wirtz D 2015 Three-dimensional matrix fiber alignment modulates cell migration and MT1-MMP utility by spatially and temporally directing protrusions *Sci. Rep.* **5** 14580
- Kim Y, Roh S, Park J, Kim Y, Cho D H and Kim J C 2009 Differential expression of the LOX family genes in human colorectal adenocarcinomas *Oncol. Rep.* **22** 799–804
- Kirschmann D A, Seftor E A, Fong S F T, Nieva D R C, Sullivan C M, Edwards E M, Sommer P, Csiszar K and Hendrix M J C 2002 A molecular role for lysyl oxidase in breast cancer invasion *Cancer Res.* **62** 4478–83
- Levental K R *et al* 2009 Matrix crosslinking forces tumor progression by enhancing integrin signaling *Cell* **139** 891–906
- Lu P, Weaver V M and Werb Z 2012 The extracellular matrix: a dynamic niche in cancer progression *J. Cell Biol.* **196** 395–406
- Mutyal N N, Radosevich A, Tiwari A K, Stypula Y, Wali R, Kunte D, Roy H K and Backman V 2013 Biological mechanisms underlying structural changes induced by colorectal field carcinogenesis measured with low-coherence enhanced backscattering (LEBS) spectroscopy *PLoS One* **8** e57206
- Naba A, Clauser K R, Whittaker C A, Carr S A, Tanabe K K and Hynes R O 2014 Extracellular matrix signatures of human primary metastatic colon cancers and their metastases to liver *BMC Cancer* **14** 518
- Nadiarynk O, LaComb R B, Brewer M A and Campagnola P J 2010 Alterations of the extracellular matrix in ovarian cancer studied by second harmonic generation imaging microscopy *BMC Cancer* **10** 94
- Nelson C M and Bissell M J 2006 Of extracellular matrix, scaffolds, and signaling: tissue architecture regulates development, homeostasis, and cancer *Annu. Rev. Cell Dev. Biol.* **22** 287–309
- Peddareddigari V G, Wang D and Dubois R N 2010 The tumor microenvironment in colorectal carcinogenesis *Cancer Microenviron.* **3** 149–66
- Pickup M W, Mouw J K and Weaver V M 2014 The extracellular matrix modulates the hallmarks of cancer *EMBO Rep.* **15** 1243–53
- Rucker R B, Kosonen T, Clegg M S, Mitchell A E, Rucker B R, Uriu-Hare J Y and Keen C L 1998 Copper, lysyl oxidase, and extracellular matrix protein cross-linking *Am. J. Clin. Nutr.* **67** 996S–1002S
- Slaughter P, Southwick W and Smejkal W 1953 'Field cancerization' in oral stratified squamous epithelium *Cancer* **6** 963–8
- Stoller P, Reiser K M, Celliers P M and Rubenchik A M 2002 Polarization-modulated second harmonic generation in collagen *Biophys. J.* **82** 3330–42
- Stypula-Cyrus Y, Damania D, Kunte D P, Cruz M D, Subramanian H, Roy H K and Backman V 2013 HDAC up-regulation in early colon field carcinogenesis is involved in cell tumorigenicity through regulation of chromatin structure *PLoS One* **8** e64600
- Tse J M, Cheng G, Tyrrell J A, Wilcox-Adelman S A, Boucher Y, Jain R K and Munn L L 2012 Mechanical compression drives cancer cells toward invasive phenotype *Proc. Natl Acad. Sci. USA* **109** 911–6
- Yi J and Backman V 2012 Imaging a full set of optical scattering properties of biological tissue by inverse spectroscopic optical coherence tomography *Opt. Lett.* **37** 4443–5

- Yi J, Radosevich A J, Rogers J D, Norris S C P, Çapoğlu İ R, Taflove A and Backman V 2013 Can OCT be sensitive to nanoscale structural alterations in biological tissue? *Opt. Express* **21** 1642–5
- Yi J, Stypula-Cyrus Y, Blaha C, Roy H K and Backman V 2015 Fractal characterization of chromatin decompaction in live cells *Biophys. J.* **109** 2218–26
- Yi J *et al* 2014 Spatially resolved optical and ultrastructural properties of colorectal and pancreatic field carcinogenesis observed by inverse spectroscopic optical coherence tomography *J. Biomed. Opt.* **19** 36013
- Zhuo S, Chen J, Xie S, Hong Z and Jiang X 2009 Extracting diagnostic stromal organization features based on intrinsic two-photon excited fluorescence and second-harmonic generation signals *J. Biomed. Opt.* **14** 020503
- Zou X *et al* 2013 Up-regulation of type I collagen during tumorigenesis of colorectal cancer revealed by quantitative proteomic analysis *J. Proteomics* **94** 473–85